

Update Combined Upper Limit on Standard Model Higgs Boson Production at CDF for 1 fb⁻¹ Data

P. Fernandez, N. Krumnack, T. Masubuchi, J. Nielsen, A. Taffard,
W. Yao
For Higgs Working Group

Abstract

This note describes an updated combination of several searches for Standard Model Higgs boson production at CDF using a data sample of 1 fb⁻¹ of integrated luminosity. The channels considered are $WH \rightarrow l\nu b\bar{b}$, $ZH \rightarrow \nu\bar{\nu} b\bar{b}$, $ZH \rightarrow l^+l^- b\bar{b}$, and $gg \rightarrow H \rightarrow W^+W^-$. All the results have been recently updated for 1 fb⁻¹ for the first time. We have calculated combined upper limits on the ratio of Higgs boson cross section times the branching ratio to its Standard Model prediction (R_{95}) for Higgs boson masses between 110 and 200 GeV/c². The results are in a good agreement with the expectations obtained from pseudo-experiments. We have also recomputed upper limits for each individual channel using the same technique as a consistent check and are able to reproduce the blessed results over all the channels. The 95% CL upper limits observed (expected) are a factor of 14.8(8.5) and 3.2(5.1) away from the Standard Model cross section for Higgs boson mass 115 and 160 GeV/c².

1 Introduction

CDF has made several searches for the Standard Model Higgs boson production using a data sample up to 1 fb⁻¹ of integrated luminosity [1] [2] [3] [4] [5] [6]. Clearly it is necessary to combine the results of all the channels to maximize the search sensitivity. The most sensitive channels are $WH \rightarrow l\nu b\bar{b}$, $ZH \rightarrow \nu\bar{\nu} b\bar{b}$, and $ZH \rightarrow l^+l^- b\bar{b}$ in the low mass range, and $g\bar{g} \rightarrow H \rightarrow W^+W^- \rightarrow l^+l^- \nu\bar{\nu}$ in the high mass range. For the combination, we follow the same procedure that was used in the Higgs combination

analysis for summer 2006 [7], which is a Bayesian framework that would allow us to handle the systematic properly on the large number of background and efficiency parameters involved.

This note is organized as follows. In section 2, we will briefly describe the combination results including the method and systematic correlations. In section 3, we will discuss the expected limits. Finally, we will conclude in section 4.

2 Combination Results

In order to combine channels with different decay modes, we are assuming that the relative rates of SM Higgs boson production between WH , ZH and $gg \rightarrow H \rightarrow W^+W^-$ are the same as SM expectations even though they can all scale up or down together. So, we can combine the limits on the ratio of Higgs boson production cross section times the branching ratio to the SM value. The statistical method employed here is a Bayesian framework, that is the same technique used in the Run1 Higgs combination [8]. For a given Higgs boson mass, the combined likelihood is a product of likelihood in the individual channels, each of which is a product over histogram bins of Poisson densities

$$\mathcal{L}(R, \vec{s}, \vec{b} | \vec{n}) = \prod_{i=1}^{N_C} \prod_{j=1}^{Nbins} \mu_{ij}^{n_{ij}} e^{-\mu_{ij}} / n_{ij}!,$$

where the prior densities for all the parameters in the likelihood are background normalization (\vec{b}), expected Standard Model signal ($\vec{s} = \sigma_{SM} \times B \times L \times \vec{\epsilon}$), luminosity (L), acceptance $\vec{\epsilon}$, and the ratio $R = \sigma \times B / (\sigma_{SM} \times B_{SM})$. The first product is over the number of channels (N_C), the second product is over histogram bins with observed data events (n_{ij}) in either dijet mass for WH and $ZH \rightarrow \nu\bar{\nu}b\bar{b}$, 2-d neural network outputs for $ZH \rightarrow l^+l^-b\bar{b}$ or likelihood of matrix element for WW . The parameters that contribute to the expected bin contents are $\mu_{ij} = R \times s_{ij} + b_{ij}$ for the channel i and the histogram bin j .

The Standard Model Higgs boson production cross sections at the Tevatron and the decay branching ratios are obtained from the Tev4LHC Higgs working group [9] and HDECAY [10], which are summarized in Table 1 as function of Higgs boson masses. The residual theoretical uncertainties for WH and ZH production cross section are rather small, less than 5%. Also there is about 10% for gluon fusion $gg \rightarrow H$ process.

Systematic uncertainties in the various analyzes come from Monte Carlo modeling of the geometrical and kinematic acceptance, btag efficiency scale factor, lepton identification, the effect due to the jet energy scale, background uncertainties, and the uncertainty on the luminosity. We divide these systematics into several groups.

- Signal acceptance: luminosity, btag efficiency scale factor, lepton identification, the jet energy scale, MC modeling (ISR/FSR+PDF), and the rest of the uncertainties.

Mass (GeV/c ²)	σ_{WH} (fb)	σ_{ZH} (fb)	σ_{WW} (fb)	$B(H \rightarrow bb)$ (%)	$B(H \rightarrow W^+W^-)$ (%)
110	207.70	123.33	1281	77.02	4.41
115	178.08	106.70	1099	73.22	7.97
120	152.89	92.70	1006	67.89	13.20
130	114.51	70.38	801	52.71	28.69
140	86.00	54.20	646	34.36	48.33
150	66.14	41.98	525	17.57	68.17
160	51.03	32.89	431	4.00	90.11
170	38.89	26.12	357	0.846	96.53
180	31.12	20.64	297	0.541	93.45
190	24.27	16.64	249	0.342	77.61
200	19.34	13.46	211	0.260	73.47

Table 1: The (N)NLO production cross sections and the decay branching ratios as function of Higgs boson masses.

- Background normalization: heavy flavor fraction, mistags, top contributions, non-W, diboson and the rest of the backgrounds. In order to treat the backgrounds in ZH channel properly, we have divided most backgrounds into two parts: one is correlated among the channels due to common systematic(luminosity, btagging, the jet energy scale and Monte Carlo modeling), the second is uncorrelated due to limited Monte Carlo statistics.
- Background shape uncertainties are estimated using pseudo-experiment with different input shapes that results in changes of expected limit. We treat it as part of systematic uncertainties on the signal, which effectively smears the final likelihood.

For each group, we assign each measurement to be 100% correlated or uncorrelated with other measurements. The breakdown of systematic for each channel are summarized in Table 2 where a positive value indicates 100% correlated systematic among the channels and a negative value indicates the systematic uncorrelated. The priors used are truncated Gaussian densities constraining a given parameter to its expected value with its uncertainty.

Since there is nothing known about the Higgs boson production cross section, we assign a flat prior to the total number of Higgs boson events $R \times s_{tot}$, instead of the cross section. The posterior density function becomes

$$p(R|\vec{n}) = \int d\vec{s} \int d\vec{b} \mathcal{L}(R, \vec{s}, \vec{b}|\vec{n}) \times s_{tot} / \int dR \int d\vec{s} \int d\vec{b} \mathcal{L}(R, \vec{s}, \vec{b}|\vec{n}) \times s_{tot},$$

where $s_{tot} = \sum_{i=0}^{Nc} \sum_{j=0}^{Nbins} s_{ij}$.

Channels	$l\nu bb$		$\nu\bar{\nu}bb$		l^+l^-bb		W^+W^-	
	ST	DT	ST	DT	ST	DT	HS/B	LS/B
Acceptance								
Luminosity (%)	6.0	6.0	6.0	6.0	6.0	6.0	6.0	6.0
btag SF (%)	5.3	16.0	4.3	8.7	5.3	16	0.0	0.0
Lepton ID (%)	2.0	2.0	2.0	2.0	1.	1.	1.5	1.5
JES (%)	3.0	3.0	(1-26)	(1.6-25)	3.0	3.0	0.0	0.0
MC modeling (%)	4.0	10.0	3.0	3.0	3.0	3.0	2.2	2.2
Trigger (%)	0.0	0.0	3.0	3.0	0.0	0.0	0.0	0.0
Backgrounds								
Mistag (%)	22	15	13	-28	24	17	0.0	0.0
QCD (%)	17	20	-7	-32	-50	-50	-0.23	-0.34
W/Z+HF(I) (%)	33	34	40	40	40	40	0	0
W+HF(II) (%)	0	0	-5	-20	0	0	0	0
Z+HF(II) (%)	0	0	-4	-11	0	0	0	0
Top(I) (%)	13.5	20	11	11	20	20	15	15
Top(II) (%)	0.	0.	-2	-3	0	0	0	0
Diboson(I) (%)	16	25	12	12	20	20	10	10
Diboson(II) (%)	0	0	-4	-9	0	0	0	0

Table 2: The breakdown of systematic uncertainties for each individual channel where the positive values mean correlated between the channels while the negative ones are uncorrelated with the rest of channels.

The corresponding 95% credibility upper limit R_{95} is

$$\int_0^{R_{95}} p(R|\vec{n})dR = 0.95.$$

The posterior densities for all channels combined are shown in Figure 1 and Figure 2 for Higgs boson mass between 110 and 200 GeV/c² where the arrows indicate the 95% credibility upper limit R_{95} . Figure 3 and Table 3 summarizes the limits from each individual channel and all the channels combined as function of Higgs boson masses.

As a check of the robustness of our calculation, we repeated the calculation by treating most systematics uncorrelated, except the luminosity and btag efficiency scale factor. This results in almost identical combined upper limits, shown in Table 4 as “uncorrelated”, which indicates that the impact of correlations are small at the present time.

3 Expected Upper Limit

To check the sensitivity of different channels, we calculate the mean upper limits one would obtain from a large ensemble of experiments. In the absence of Higgs boson

mh	110	115	120	130	140	150	160	180
$H\nu bb$	25.8	27.2	25.8	27.2	46.2	115.2		
Expected	14.6	17.2	20.1	30.0	57.9	138.4		
$H\nu\bar{\nu}bb$	18.2	21.2	25.2	39.8	67.2			
Expected	13.0	15.1	17.4	26.0	47.3			
Hl^+l^-bb	16.2	17.8	19.8	32.8	73.8	185.2		
Expected	16.4	18.2	20.7	31.0	62.6	164.0		
HWW	143.2	66.8	31.8	15.8	9.2	5.8	3.2	7.2
Expected	132.9	57.8	38.4	18.6	11.9	8.3	5.1	7.0

Table 3: The summary of observed, expected limits from each individual channel as function of Higgs boson masses.

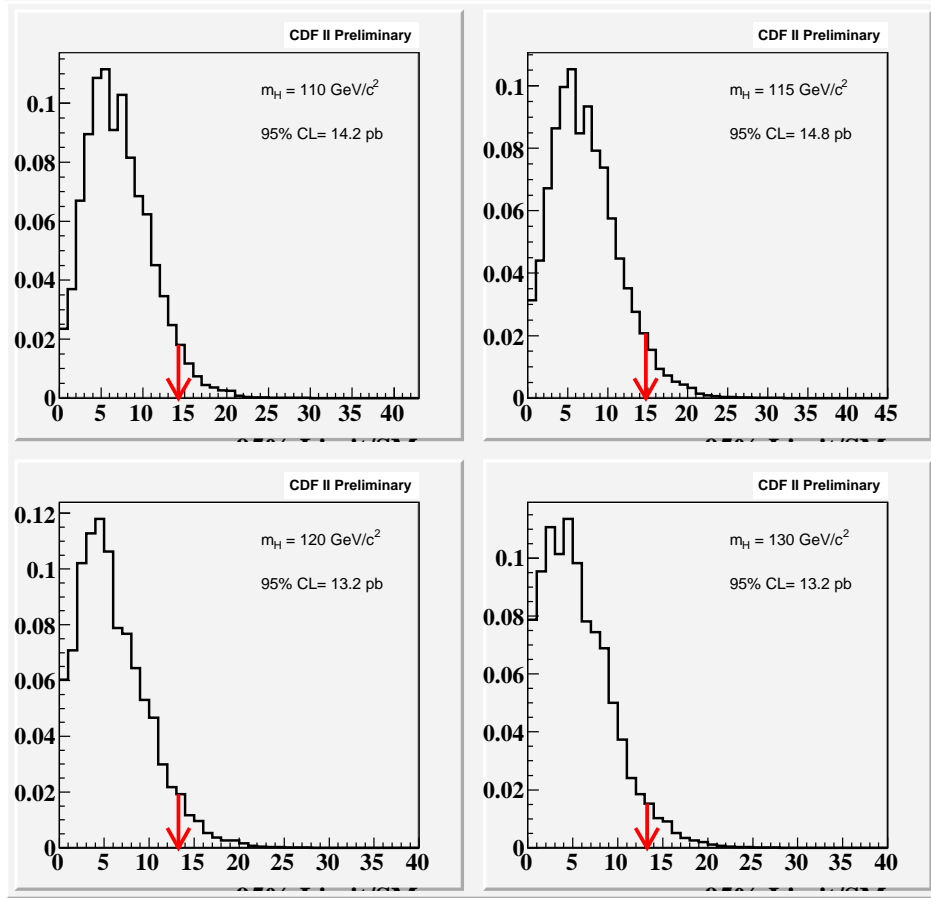


Figure 1: The posterior densities for all channels combined for Higgs boson mass between 110 and 130 GeV/c^2 where the arrows indicate the 95% credibility upper limit R_{95} .

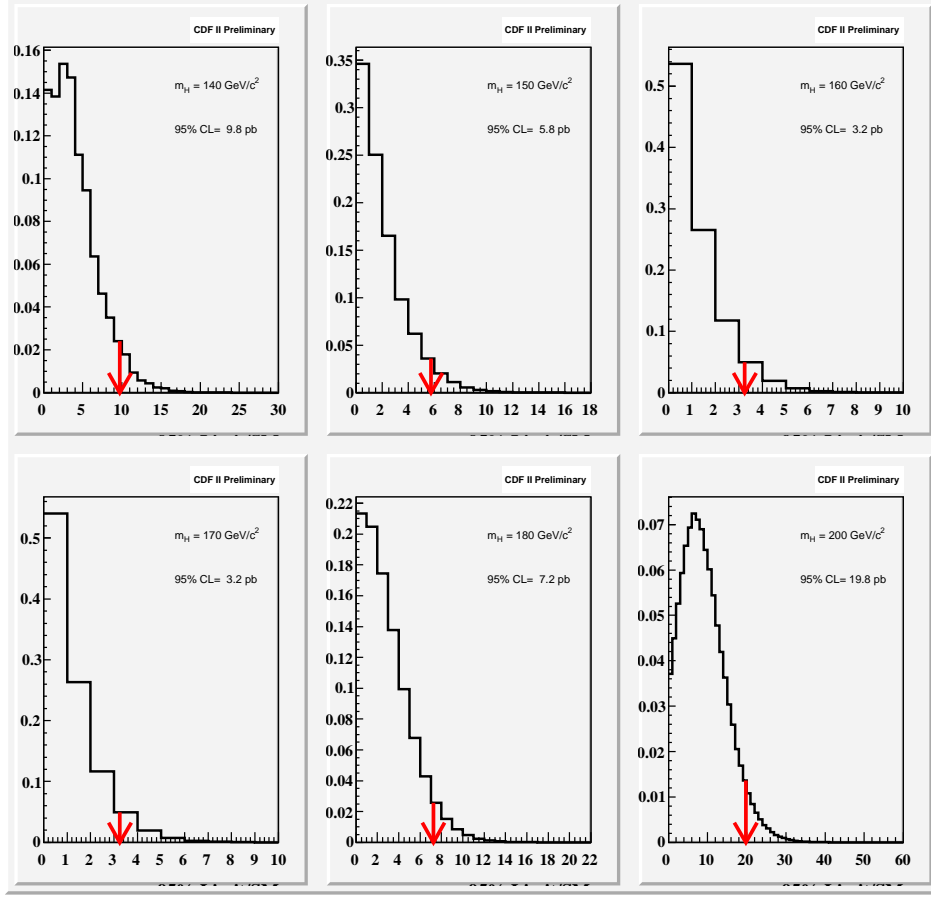


Figure 2: The posterior densities for all channels combined for Higgs boson mass between 140 and 200 GeV/c^2 where the arrows indicate the 95% credibility upper limit R_{95} .

signal, the pseudo-experiment is generated by fluctuating the expected backgrounds with their uncertainties. Figure 4 and Figure 5 show the distributions of upper limits from the pseudo-experiments for various Higgs boson masses. The observed upper limits from data are also shown by the red arrows, which are consistent with the expectation of pseudo-experiments.

The final combined limit and its expectation are listed in Table 4, which are also in good agreement with the results reported in cdfnote 8784 /citetom.

4 Conclusions

We have described an updated combination of several searches for Standard Model Higgs boson production at CDF using a data sample of 1 fb^{-1} of integrated luminosity. The channels considered are $WH \rightarrow l\nu b\bar{b}$, $ZH \rightarrow \nu\bar{\nu} b\bar{b}$, and $gg \rightarrow H \rightarrow W^+W^-$.

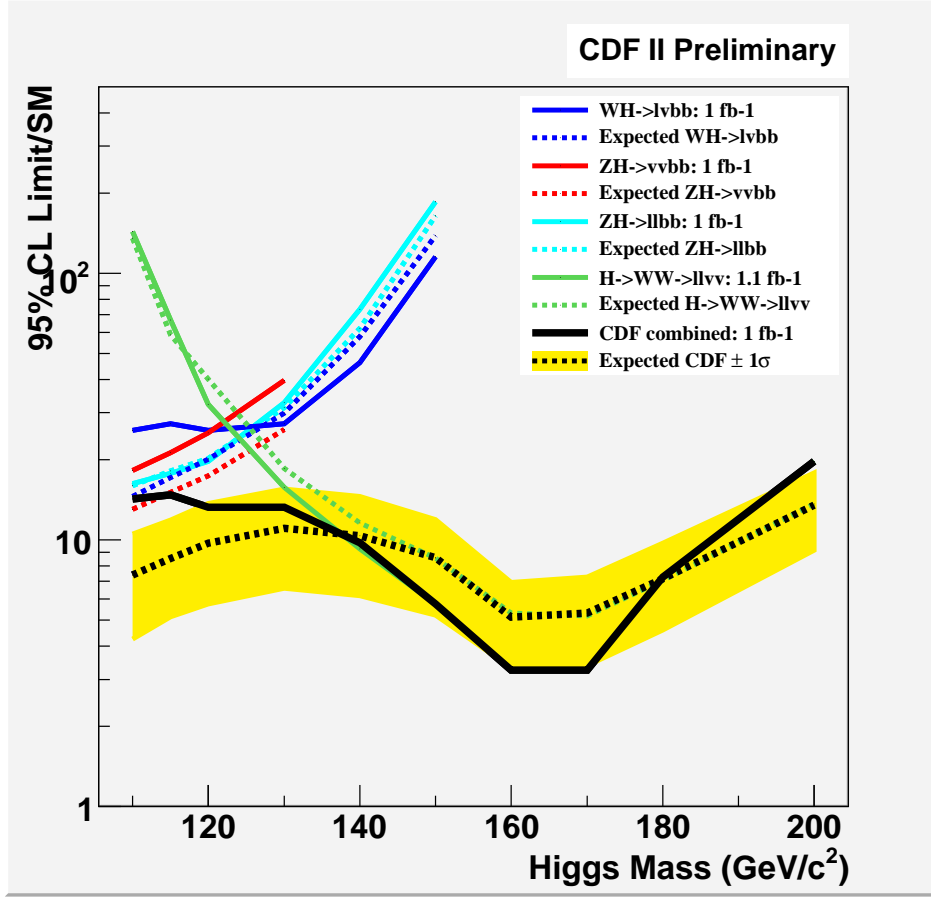


Figure 3: The combined upper limit as function of Higgs boson masses between 110 and 200 GeV/c^2 as well as the individual limits from individual channels.

We have calculated combined upper limits on the ratio of Higgs boson cross section times the branching ratio to its Standard Model prediction (R_{95}) for Higgs boson masses between 110 and 200 GeV/c^2 . The results are in a good agreement with the expectations obtained from pseudo-experiments. We have also recomputed upper limits for each individual channel using the same technique as a consistent check and are able to reproduce the blessed results over all the channels. The 95% CL upper limits observed (expected) are a factor of 14.8 (8.5) and 3.2(5.1) away from the Standard Model cross section for Higgs boson mass 115 and 160 GeV/c^2 .

5 Acknowledgments

We thank Ben Kilminster, Viktor Veszpremi, and Shih-Chieh Hsu for providing the results of their analysis, which makes this combination possible.

Mass (GeV/c ²)	Combined Limit		Expected Limit	
	Correlated	Uncorrelated	Mean	RMS
110	14.2	13.8	7.4	3.1
115	14.8	12.8	8.5	3.4
120	13.2	11.8	9.7	4.0
130	13.2	11.2	11.1	4.5
140	9.8	14.8	10.4	4.2
150	5.8	11.8	8.6	3.3
160	3.2	10.2	5.1	1.8
170	3.2	12.2	5.3	1.9
180	7.2	18.2	7.2	2.6
200	19.8	40.8	13.5	4.3

Table 4: The summary of observed, expected limits for various Higgs boson masses.

References

- [1] Y. Kusakabe et al, Search for Standard Model Higgs Boson Production in Association with W Boson at CDF with 1 fb⁻¹, CDF Note 8390 and 8355;
Y. Kusakabe et al, Search for Standard Model Higgs Boson Production in Association with W[±] Boson at CDF with 695 pb⁻¹, CDF Note 8194. 1
- [2] V. Veszpremi et al, Search for the Standard Model Higgs Boson in the Missing Et and b-jet Signature, CDF Note 8442 and 8362;
V. Veszpremi et al, Search for the Standard Model Higgs Boson in the ZH→ $\nu\bar{\nu}b\bar{b}$ channel, CDF Note 7719. 1
- [3] J. Efron et al, Search for $ZH \rightarrow l^+l^-b\bar{b}$ in 1 fb⁻¹ of CDF Run 2 Data, CDF Note 8742 and 8704;
J. Efron et al, Search for $ZH \rightarrow l^+l^-b\bar{b}$ in 1 fb⁻¹ of CDF Run 2 Data, CDF Note 8422 and 8363. 1
- [4] Shih-Chieh Hsu et al, Search for HWW Production with Matrix Element Methods Using 1.1fb⁻¹, CDF Note 8774 and 8719;
S. Chuang, M. Coca, and M. Kruse, Search for a SM Higgs Boson in the $gg \rightarrow H \rightarrow WW^*$ Dilepton Channel with 360 pb⁻¹ Run II Data, CDF Note 7708. 1
- [5] S. Lai and P. Sinervo, Search for ttH production - Result, CDF Note 8203. 1
- [6] H. Kobayashi, K. Yamamoto, and Y. Seiya, Search for the WH Production Using High-Pt Isolated Like-Sign Dilepton Events in Run II, CDF Note 7262. 1
- [7] Y. Kusakabe et al, Combined Upper Limit on Standard Model Higgs Boson Production at CDF for Summer 2006, CDF Note 8403, 8326, and 8276. 2

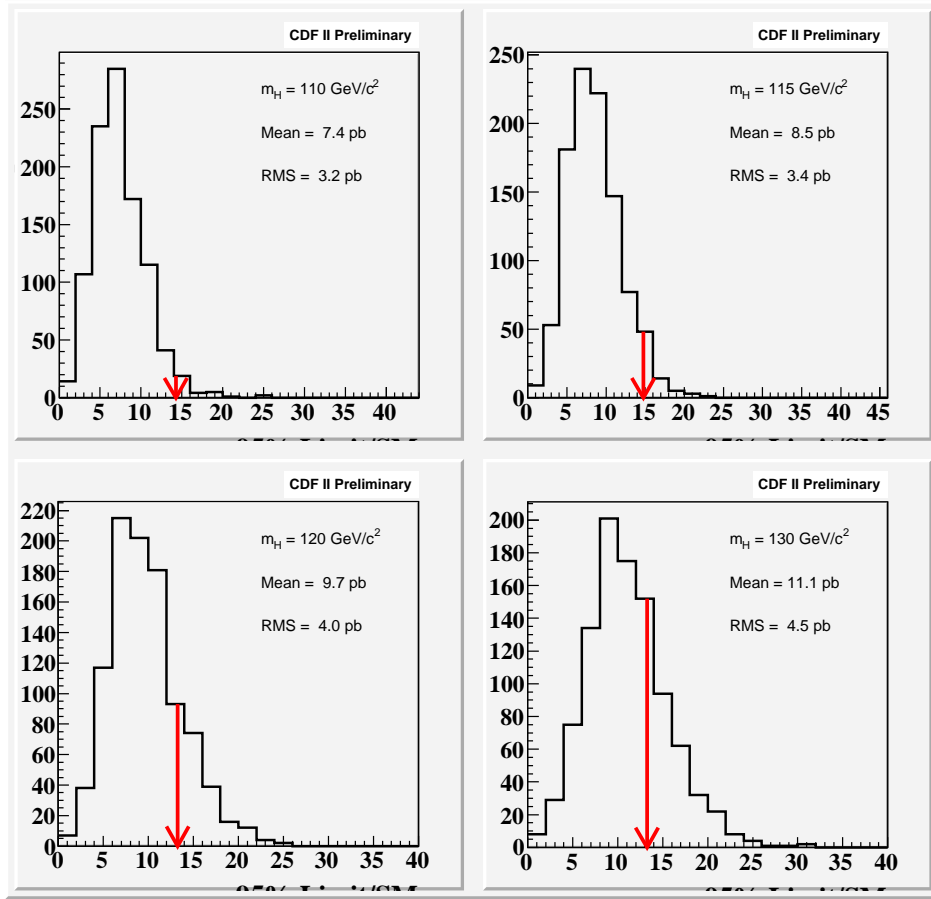


Figure 4: The distributions of upper limits from the pseudo-experiments for Higgs boson mass between 110 and 130 GeV/c^2 where the arrows indicate the observed 95% upper limit from data.

- [8] L. Demortier, M. Kruse, J. Valls, and W. Yao, Combined Upper Limits on Run I Higgs Production, CDF Note 4985. 2
- [9] TeV4LHC Higgs working group at <http://maltoni.home.cern.ch/maltoni/TeV4LHC/SM.html>. 2
- [10] A. Djouadi, J. Kalinowski, and M. Spira, Comp. Phys. Commun. 108 C (1998) 56. 2
- [11] T. Junk, Combined Upper Limit on Standard Model Higgs Boson Production for Spring 2007, CDF Note 8784

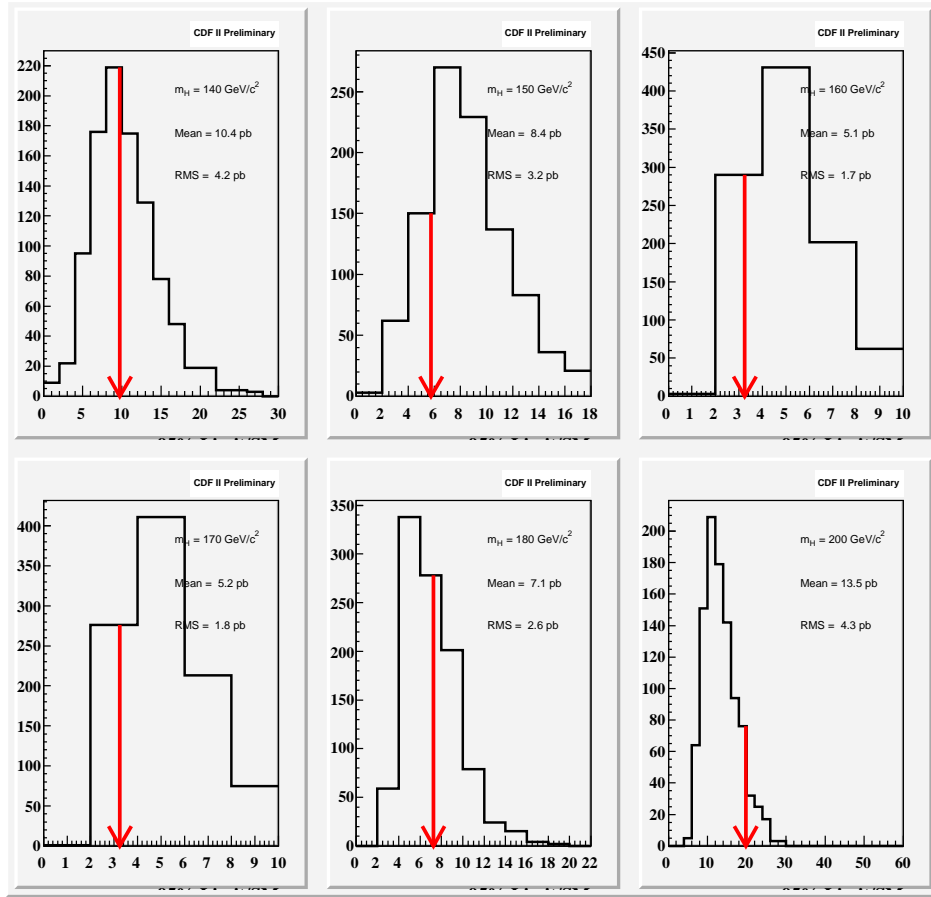


Figure 5: The distributions of upper limits from the pseudo-experiments for Higgs boson mass between 140 and 200 GeV/c^2 where the arrows indicate the observed 95% upper limit from data.